CrossMark

ARTICLE

Indocyanine green-incorporated exosomes for improved in vivo imaging of sentinel lymph node

Gyeonghui Yu[1] · Heesun Jung[1] · Hyejung Mok[1]

Abstract For improved physical stability and fast accumulation in sentinel lymph nodes in vivo, indocyanine green (ICG) was incorporated into exosomes (EXOs) to form a novel ICG-based near-infrared fluorescence probe. Compared with free ICG, prepared ICG-TBAI-encapsulated EXOs (ICG/EXOs) smaller than 50 nm had greater physicochemical stability in aqueous solution when exposed to light at 37 °C. In addition, sentinel lymph nodes were visualized within minutes with ICG/EXOs at a low ICG dose (0.05 mg/kg) owing to its well-controlled size distribution. Taken together, the results show that ICG/EXOs are effective biocompatible and sensitive near-infrared probes for real-time sentinel lymph node imaging in vivo.

Keywords Exosome · Indocyanine green · In vivo imaging · Sentinel lymph node

Introduction

Biocompatible probes with strong fluorescence intensities (FIs) and low background signals at sites of detection are essential for optical diagnosis and imaging in vivo. Indocyanine green (ICG) is a widely used FDA-approved near-infrared fluorescence probe for sentinel lymph node biopsy during surgery (Desmettre et al. 2000; Chi et al. 2013; Watkin and La-Touche 2014). However, external factors such as light and temperature can lessen the FI of ICG in vivo (Engel et al. 2008). Accordingly, ICG has been formulated into nanosized particles and hydrogels for enhanced stability in aqueous solution (Mok et al. 2012; Kim et al. 2014).

Exosomes (EXOs) have a natural phospholipid bilayer composed of cholesterol, sphingolipids, glycerophospholipids, and ceramide (Caradec et al. 2014). They are released from cells into diverse body fluids such as plasma, saliva, and urine via exocytosis (Tan et al. 2013; Caradec et al. 2014; Johnsen et al. 2014). Exosomal proteins and genes have crucial biological functions, including immune modulation, tumor progression, induction of angiogenesis, cell invasion, and metastasis (Tan et al. 2013; Caradec et al. 2014; Villarroya-Beltri et al. 2014). Recently, EXOs with hydrodynamic sizes of approximately 30–100 nm have been harnessed not only as nature-derived nanomaterials for the delivery of small molecules and small interfering RNAs but also as diagnostic biomarkers (Sun et al. 2010; Alvarez-Erviti et al. 2011; Johnsen et al. 2014). Given that the hydrodynamic size of particles is critical for in vivo distribution and successful localization in sentinel lymph nodes, EXOs may be appropriate carriers for the efficient delivery of therapeutic molecules and imaging agents to lymphatic systems and tumor tissues (Cabral et al. 2011; Noh et al. 2012). However, to the best of our knowledge, EXO-based probes have not yet been studied for lymph node imaging.

In this study, ICG was incorporated into EXOs, and the combination was evaluated for real-time imaging of sentinel lymph nodes. Optimal loading efficiency and hydrodynamic size were determined for ICG-loaded EXOs. In addition, fluorescence stability and optimal hydrodynamic size for long-term incubation were examined in aqueous solutions. Furthermore, ICG-tetrabutylammonium iodide

✉ Hyejung Mok
hjmok@konkuk.ac.kr

[1] Department of Bioscience and Biotechnology, Konkuk University, Seoul 05029, Republic of Korea

(TBAI) and ICG-TBAI-encapsulated EXOs (ICG/EXOs) were administered to mice forepaws via transdermal injection, and fluorescence imaging was monitored in real-time with an in vivo imaging instrument.

Materials and methods

Materials

Fetal bovine serum (FBS) was purchased from Gibco BRL (USA). An Exo-Quick TC EXO precipitation kit was obtained from SBI System Biosciences, Inc. (USA). ICG (cardiogreen polymethine dye, molecular weight, 775) was purchased from Dongindang Pharmaceutical (Korea). TBAI was obtained from Sigma Aldrich (USA). A microbicinchoninic acid (BCA) protein quantitation assay kit and desalting column (molecular weight cut-off [MWCO], 40 kDa) were purchased from Thermo Scientific (USA). Six-week-old female Balb/C mice were purchased from Orient Bio Inc. (Korea).

Preparation of ICG/EXOs

The EXOs in this study were isolated from FBS according to the manufacturer's protocol. FBS (1 mL) was mixed with ExoQuick-TC EXO precipitation solution (200 μL) via inversion. After incubation at 4 °C overnight, the mixture was centrifuged at $1500 \times g$ for 30 min. After additional centrifugation at $1500 \times g$ for 5 min, the pellet was resuspended with phosphate-buffered saline (PBS) solution and stored at 4 °C. The amount of protein in the EXOs was determined using the BCA protein assay kit according to the manufacturer's protocol. For facile encapsulation of ICG by EXOs, hydrophobic ICG-TBAI salt was prepared as previously reported (Kim et al. 2010). ICG (16 mg) was mixed with TBAI (46 mg) at an ICG/TBAI molar ratio of 1/6 in methanol. After evaporation of methanol, ICG-TBAI complex was dissolved in DMSO for further experiments.

Characterization of ICG/EXOs

EXOs (protein amount, 40 μg) were mixed with ICG-TBAI at various ICG amounts of 0, 2, 4, and 20 μg (ICG/exosomal protein weight ratios of 0, 0.05, 0.1, and 0.5, respectively) at 37 °C for 2 h. After incubation, free ICG-TBAI was removed with a desalting column (MWCO, 40 kDa). The hydrodynamic size of the ICG/EXOs at each weight ratio was measured with dynamic light scattering (DLS; Malvern Instruments Ltd., UK). For encapsulation efficiency determination, EXOs (protein amount, 40 μg) were mixed with ICG-TBAI at ICG/exosomal protein

weight ratios of 0.05, 0.1, and 0.2 at 37 °C for 2 h. After purification with the desalting column, the fluorescent intensities of the ICG/EXO solutions were measured with an IVIS imaging system (Lumina II; Caliper Life Sciences, USA) at excitation and emission wavelengths of 780 and 831 nm, respectively. The relative encapsulation efficiency was calculated as follows: [amount of ICG in EXOs]/[amount of feed ICG] $\times$ 100.

Stability testing of ICG/EXOs

EXOs (protein amount, 40 μg) were mixed with ICG-TBAI at an ICG/exosomal protein weight ratio of 0.1 at 37 °C for 2 h. After incubation, free ICG-TBAI was removed with a desalting column (MWCO, 40 kDa). Three types of samples including free ICG, free ICG-TBAI, and ICG/EXO at an ICG concentration of 1 μM were incubated at 37 °C for predetermined times (0, 3, 6, and 20 h) in the presence of light. FIs were measured with the IVIS imaging instrument at excitation and emission wavelengths of 780 and 831 nm, respectively. Relative FI was calculated as follows: [FI after incubation]/[initial FI at 0 h] $\times$ 100. To examine changes in EXO and ICG/EXO particle sizes, we incubated two types of EXOs in PBS solution for 4 days at 4 °C and used DLS to measure particle size at predetermined times.

Sentinel lymph node imaging

For in vivo monitoring of ICG/EXOs, six-week-old female Balb-c nude mice were anesthetized with an intraperitoneal injection of Rompun/Zoletil according to the manufacturer's protocol. Then, free ICG-TBAI and ICG/EXOs were injected into the forepaws of the mice at a low dose (0.05 mg/kg) and a high dose (0.3 mg/kg) of ICG. After the injection of the ICG-based samples and incubation for predetermined times (1, 5, 10, 30, 60, and 120 min and 24 h), fluorescence images of each mouse were obtained with the IVIS imaging system. The total flux of whole mice forepaws was also quantitatively analyzed with the IVIS imaging system.

Results and discussion

ICG/EXOs preparation

After the isolation of EXOs from FBS, the amount of isolated exosomal protein was quantified with a BCA assay (Twu et al. 2013). The total amount of protein in the EXOs in PBS solution with detergent (1 % Tx-100) was similar to that in EXOs in solution without detergent, which suggests that the total exosomal proteins in the exterior and interior regions of the EXOs were measured with the BCA assay.

We isolated 138.4 ± 7.1 mg exosomal protein from 100 µL of 100 % FBS solution.

For facile entrapment of ICG within EXOs, ICG was complexed with TBAI via ionic interactions (Kim et al. 2010). As shown in Fig. 1, exosomal protein was incubated with ICG-TBAI for 2 h at 37 °C, entrapping ICG within EXOs via hydrophobic interactions. After column purification of the resulting solution to remove free ICG-TBAI, the ICG/EXOs were administered to mice forepaws to examine the fluorescence signals in sentinel lymph nodes. In this study, we hypothesized that EXOs would be excellent vehicles for the delivery of ICG to sentinel lymph nodes due to their hydrodynamic size of approximately 50 nm with narrow size distribution after in vivo administration.

Characterization of ICG/EXOs

To determine the optimal weight ratio of ICG to exosomal protein, we incubated ICG with exosomal protein at various ICG/exosomal protein weight ratios. The hydrodynamic sizes of the resultant ICG/EXOs were examined with DLS. As shown in Fig. 2A, the EXOs exhibited a narrow size distribution with a size of 35.8 ± 3.1 nm. Although the size distribution of the ICG/EXOs at low ICG/exosomal protein weight ratios was similar to that of EXOs alone, large aggregation with broad size distribution was observed in ICG/EXOs at an ICG/exosomal protein weight ratio of 0.5. Figure 2B shows that compared with that of EXOs, the hydrodynamic size of ICG/EXOs up to an ICG/exosomal protein weight ratio of 0.2 was much larger. The sizes of ICG/EXOs at ICG/exosomal protein weight ratios of 0.5 and 0.2 were 82.4 ± 45.5 and 46.2 ± 11.1 nm, respectively. As the ICG/exosomal protein weight ratio deceased, the hydrodynamic size of the resulting ICG/EXOs decreased accordingly. The sizes of ICG/EXOs at ICG/exosomal

protein weight ratios of 0.1 and 0.05 were 40.9 ± 1.8 and 46.3 ± 14.3 nm, respectively.

The entrapment efficiency of ICG in EXOs was also examined at various ICG/exosomal protein weight ratios (Fig. 2C). The entrapment efficiencies of ICG within EXOs at ICG/exosomal protein weight ratios of 0.05, 0.1, and 0.2 were 5.4 ± 2.6, 14.0 ± 4.3, and 13.0 ± 4.2 %, respectively. Taken together, ICG/EXOs were prepared at an ICG/exosomal protein weight ratio of 0.1 for further experiments due to the small hydrodynamic size and high entrapment efficiency at this ratio.

Stability of ICG/EXOs

ICG is extremely vulnerable to external physicochemical conditions such as light, pH, and temperature (Saxena et al. 2004). The relative FIs of ICG and ICG/EXOs were examined after incubation at 37 °C in the presence of light for predetermined times (Fig. 3A). Although both free ICG and ICG-TBAI exhibited severe FI loss, the FI of ICG/EXOs was not decreased during incubation. This result indicates that the incorporation of ICG into EXOs may protect ICG from physicochemical damage from light exposure in solution.

The stability of ICG/EXOs was also determined by measuring their sizes after incubation at 4 °C for 4 days, as shown in Fig. 3B. No noticeable change in the size of the ICG/EXOs was observed for 2 days, whereas the hydrodynamic size of the ICG/EXOs gradually increased after 3 days. However, no change in the size of the EXOs occurred during incubation at 4 °C for 4 days. The non-specific aggregation of ICG/EXOs during extended incubation might be attributable to the presence of ICG on EXO surfaces. Accordingly, freshly prepared ICG/EXOs were used for the in vivo imaging of sentinel lymph nodes.
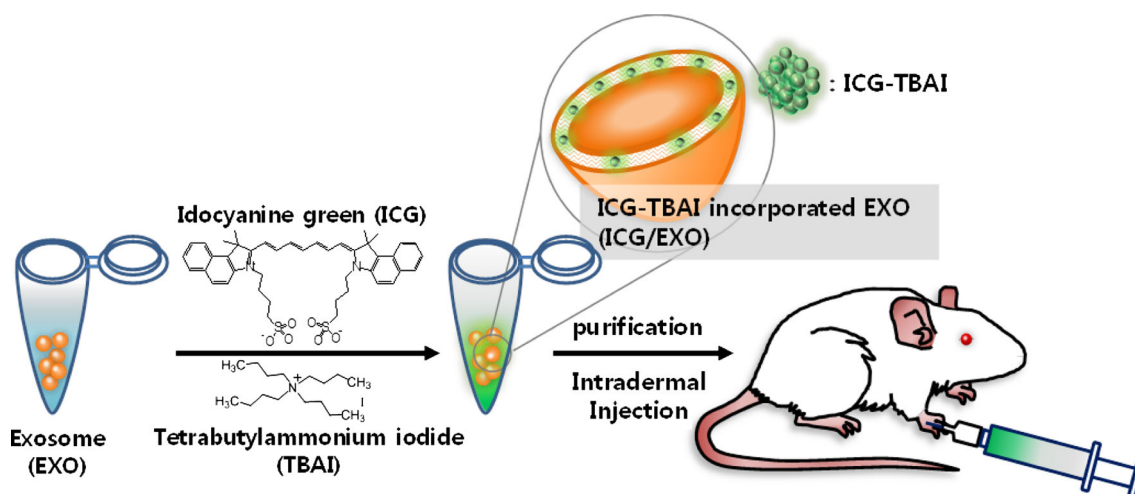

Fig. 1 Schematic illustration of preparation of ICG/EXO and in vivo administration

Fig. 2 (**A**) Size distribution of EXO and ICG/EXO at different ICG/exosomal protein weight ratios. (**B**) Hydrodynamic size and (**C**) Entrapment efficiency of ICG/EXO at different ICG/exosomal protein weight ratios
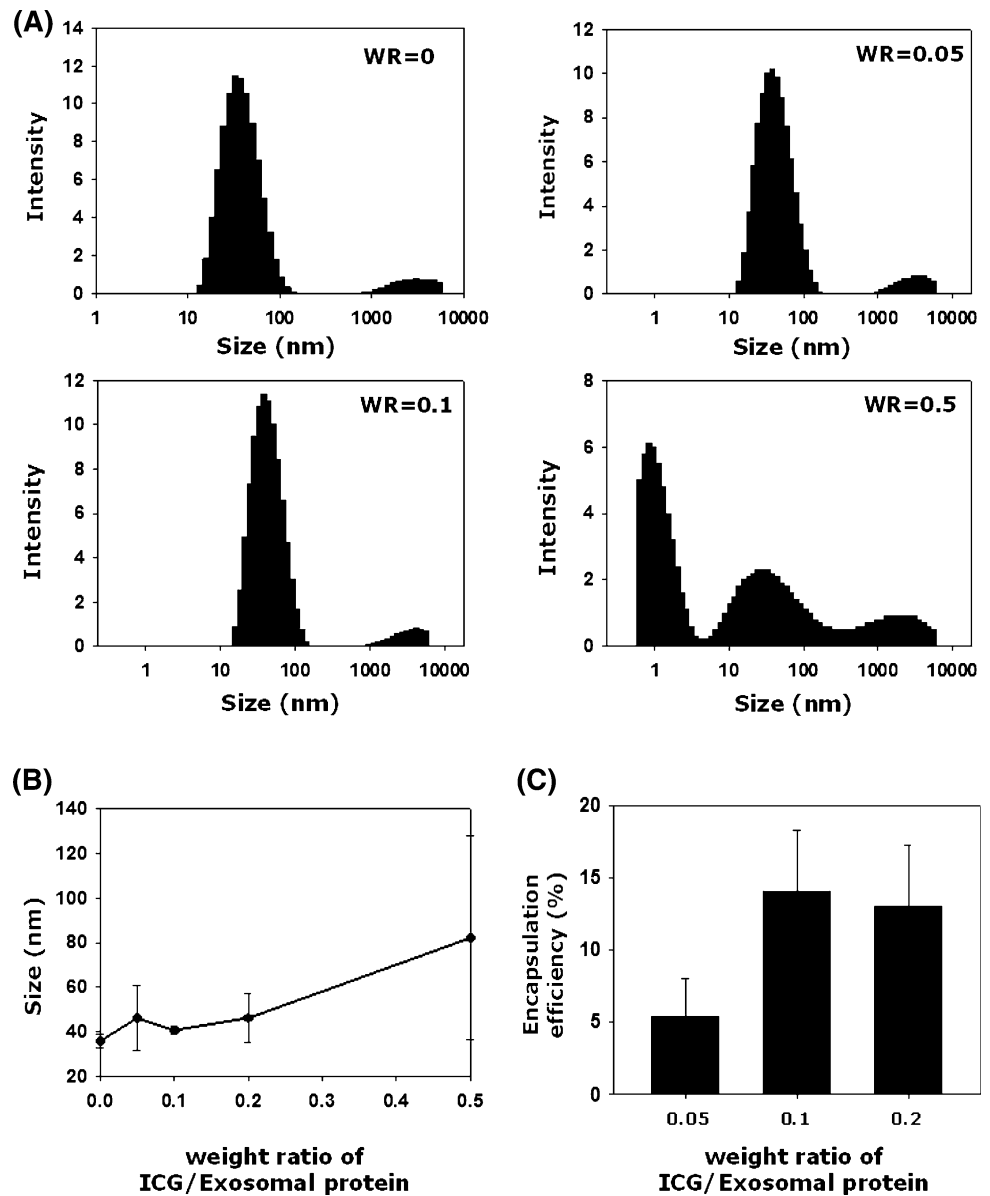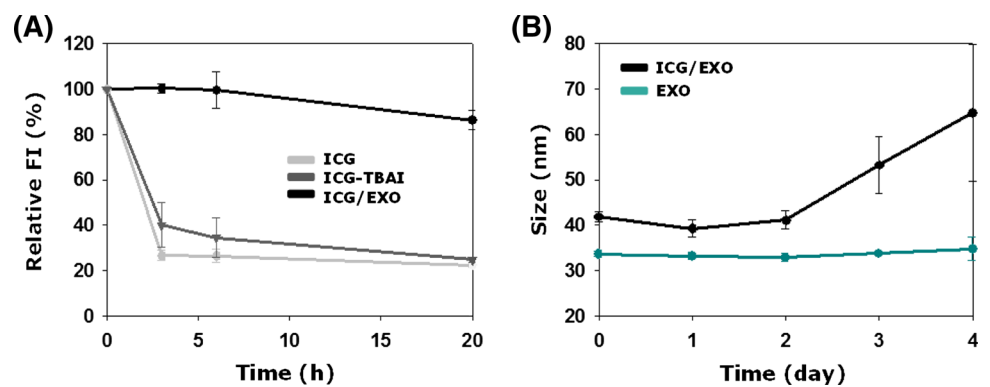

Fig. 3 (**A**) FI of ICG and ICG/EXO after incubation with exterior light exposure in aqueous solution. (**B**) Size measurement of EXO and ICG/EXO during incubation for predetermined times

Sentinel lymph node imaging with ICG/EXOs

In previous studies, ICG and formulated ICG have been administered via transdermal injection at a concentration of 0.08–1.25 mg/kg (Robinson et al. 2013). In the present study, ICG-TBAI and ICG/EXOs containing a low dose of ICG (0.05 mg/kg) were injected into mice forepaws. Fluorescence signals in sentinel lymph nodes were then monitored in real-time, as shown in Fig. 4A. As a control, ICG-TBAI containing a high dose of ICG (0.3125 mg/kg) was also administered. ICG-TBAI with low-dose ICG had a poor fluorescence signal in sentinel lymph nodes, whereas ICG/EXOs with low-dose ICG had a rapid and strong fluorescence signal. ICG-TBAI with high-dose ICG showed fluorescent signals comparable to those of ICG/EXOs with low-dose ICG.

The FIs of each lymph node were also analyzed quantitatively (Fig. 4B). The total flux measurements of gated sentinel lymph nodes were 0.4 ± 0.3, 1.9 ± 0.9, and 2.2 ± 0.8 ($\times 10^9$) photons/s after treatment with ICG-TBAI (low-dose ICG), ICG/EXOs (low-dose ICG), and ICG-TBAI (high-dose ICG), respectively, and incubation for 2 min. These results demonstrated that ICG/EXOs provide strong and fast imaging of sentinel lymph nodes with a low dose of ICG. Interestingly, mice treated with free ICG-TBAI (high-dose ICG) showed increased FI after 120 min while no change in FI was observed in mice treated with

ICG/EXOs. It might be attributed to fast translocation of ICG/EXOs into sentinel lymph nodes within several minutes, compared to free ICG-TBAI. In a previous study, particles with sizes of 10–50 nm were effective for fast translocation into sentinel lymph nodes and extended accumulation (Noh et al. 2012). ICG/EXOs with well-controlled sizes will likely allow favorable and fast localization to lymph nodes and result in clear visualization of sentinel lymph nodes at a low ICG concentration.

In this study, ICG/EXOs were fabricated as novel ICG-based near-infrared probes for real-time monitoring of sentinel lymph nodes. ICG/EXOs with a size of ∼50 nm exhibited stable FI in the presence of exterior light. In addition, ICG/EXOs containing low-dose ICG provided fast and strong visualization of sentinel lymph nodes after transdermal injection owing to their well-controlled size distribution. Taken together, the results of this study indicate that these nanosized near-infrared ICG/EXO probes could allow fast and excellent real-time monitoring of not only sentinel lymph node but also other organs and tissues, including tumors with low vascularization.

Fig. 4 (**A**) Visualization of FI in sentinel lymph nodes after administration of ICG and ICG/EXO via transdermal injection to mice forepaws. (**B**) Quantitative analysis of total flux in sentinel lymph nodes using IVIS imaging program

References

Alvarez-Erviti L, Seow Y, Yin H, Betts C, Lakhal S, Wood MJ (2011) Delivery of siRNA to the mouse brain by systemic injection of targeted exosomes. Nat Biotechnol 29(4):341–345

Cabral H, Matsumoto Y, Mizuno K, Chen Q, Murakami M, Kimura M, Terada Y, Kano MR, Miyazono K, Uesaka M, Nishiyama N, Kataoka K (2011) Accumulation of sub-100 nm polymeric micelles in poorly permeable tumours depends on size. Nat Nanotechnol 6(12):815–823

Caradec J, Kharmate G, Hosseini-Beheshti E, Adomat H, Gleave M, Guns E (2014) Reproducibility and efficiency of serum-derived exosome extraction methods. Clin Biochem 47(13–14):1286–1292

Chi CW, Ye JZ, Ding HL, He D, Huang WH, Zhang GJ, Tian J (2013) Use of indocyanine green for detecting the sentinel lymph node in breast cancer patients: from preclinical evaluation to clinical validation. PLoS One 8(12):e83927

Desmettre T, Devoisselle JM, Mordon S (2000) Fluorescence properties and metabolic features of indocyanine green (ICG) as related to angiography. Surv Ophthalmol 45(1):15–27

Engel E, Schraml R, Maisch T, Kobuch K, Koenig B, Szeimies RM, Hillenkamp J, Baumler W, Vasold R (2008) Light-induced decomposition of indocyanine green. Invest Ophthalmol Vis Sci 49(5):1777–1783

Johnsen KB, Gudbergsson JM, Skov MN, Pilgaard L, Moos T, Duroux M (2014) A comprehensive overview of exosomes as drug delivery vehicles—Endogenous nanocarriers for targeted cancer therapy. Bba-Rev Cancer 1:75–87

Kim TH, Chen Y, Mount CW, Gombotz WR, Li X, Pun SH (2010) Evaluation of temperature-sensitive, indocyanine green-encapsulating micelles for noninvasive near-infrared tumor imaging. Pharm Res 27(9):1900–1913
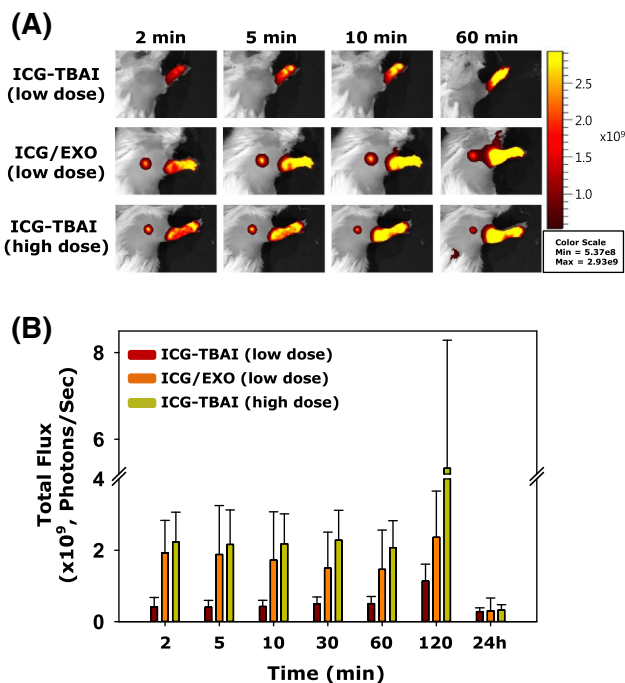
Kim J, Chong Y, Mok H (2014) Shell-crosslinked hyaluronic acid nanogels for live monitoring of hyaluronidase activity in vivo. Macromol Biosci 14(6):881–888

Mok H, Jeong H, Kim SJ, Chung BH (2012) Indocyanine green encapsulated nanogels for hyaluronidase activatable and selective near infrared imaging of tumors and lymph nodes. Chem Commun (Camb) 48(69):8628–8630

Noh YW, Kong SH, Choi DY, Park HS, Yang HK, Lee HJ, Kim HC, Kang KW, Sung MH, Lim YT (2012) Near-infrared emitting polymer nanogels for efficient sentinel lymph node mapping. ACS Nano 6(9):7820–7831

Robinson HA, Kwon S, Hall MA, Rasmussen JC, Aldrich MB, Sevick-Muraca EM (2013) Non-invasive optical imaging of the lymphatic vasculature of a mouse. J Vis Exp 73:e4326

Saxena V, Sadoqi M, Shao J (2004) Enhanced photo-stability, thermal-stability and aqueous-stability of indocyanine green in polymeric nanoparticulate systems. J Photochem Photobiol, B 74(1):29–38

Sun D, Zhuang X, Xiang X, Liu Y, Zhang S, Liu C, Barnes S, Grizzle W, Miller D, Zhang HG (2010) A novel nanoparticle drug delivery system: the anti-inflammatory activity of curcumin is enhanced when encapsulated in exosomes. Mol Ther 18(9):1606–1614

Tan A, Rajadas J, Seifalian AM (2013) Exosomes as nano-theranostic delivery platforms for gene therapy. Adv Drug Deliver Rev 65(3):357–367

Twu O, de Miguel N, Lustig G, Stevens GC, Vashisht AA, Wohlschlegel JA, Johnson PJ (2013) Trichomonas vaginalis exosomes deliver cargo to host cells and mediate hostratioparasite interactions. PLoS Pathog 9(7):e1003482

Villarroya-Beltri C, Baixauli F, Gutierrez-Vazquez C, Sanchez-Madrid F, Mittelbrunn M (2014) Sorting it out: regulation of exosome loading. Semin Cancer Biol 28:3–13

Watkin N, La-Touche S (2014) Penile cancer: developments in sentinel lymph node biopsy for penile cancer. Nat Rev Urol 11(3):135–137